Theses and Dissertations | 1. Thesis and Dissertation Collection, all items

1992-06

# Implementation of the one bit spectral correlation algorithm

## Hutcheson, George A.

Monterey, California. Naval Postgraduate School

http://hdl.handle.net/10945/23920

| REPORT DOCUMENTATION PAGE | | Form Approved OMB No 0704-0188 |
|---|---|---|

| 1a REPORT SECURITY CLASSIFICATION UNCLASSIFIED | 1b RESTRICTIVE MARKINGS |
|---|---|

| 2a SECURITY CLASSIFICATION AUTHORITY | 3 DISTRIBUTION / AVAILABILITY OF REPORT |
|---|---|
| 2b DECLASSIFICATION / DOWNGRADING SCHEDULE | Approved for public release; distribution is unlimited |

| 4 PERFORMING ORGANIZATION REPORT NUMBER(S) | 5 MONITORING ORGANIZATION REPORT NUMBER(S) |
|---|---|

| 6a NAME OF PERFORMING ORGANIZATION Naval Postgraduate School | 6b OFFICE SYMBOL (If applicable) EC | 7a NAME OF MONITORING ORGANIZATION Naval Postgraduate School |
|---|---|---|

| 6c ADDRESS (City, State, and ZIP Code) Monterey, CA 93943-5000 | 7b ADDRESS (City, State, and ZIP Code) Monterey, CA 93943-5000 |
|---|---|

| 8a NAME OF FUNDING / SPONSORING ORGANIZATION | 8b OFFICE SYMBOL (If applicable) | 9 PROCUREMENT INSTRUMENT IDENTIFICATION NUMBER |
|---|---|---|

| 8c ADDRESS (City, State, and ZIP Code) | 10 SOURCE OF FUNDING NUMBERS | | | |
|---|---|---|---|---|
| | PROGRAM ELEMENT NO | PROJECT NO | TASK NO | WORK UNIT ACCESSION NO |

11 TITLE (Include Security Classification)

IMPLEMENTATION OF THE ONE BIT SPECTRAL CORRELATION ALGORITHM

12 PERSONAL AUTHOR(S)
HUTCHESON, George A.

| 13a TYPE OF REPORT Master's Thesis | 13b TIME COVERED FROM _____ TO _____ | 14 DATE OF REPORT (Year, Month, Day) 1992 June | 15 PAGE COUNT 52 |
|---|---|---|---|

16 SUPPLEMENTARY NOTATION The views expressed in this thesis are those of the author and do not reflect the official policy or position of the Department of Defense or the US Government.

| 17 COSATI CODES | | | 18 SUBJECT TERMS (Continue on reverse if necessary and identify by block number) |
|---|---|---|---|
| FIELD | GROUP | SUB-GROUP | OBSCA, One Bit Spectral Correlation Algorithm |
| | | | |
| | | | |

19 ABSTRACT (Continue on reverse if necessary and identify by block number)

The computational efficiency of the One Bit Spectral Correlation Algorithm is compared to other cyclic spectrum analysis algorithms. A transmission bandwidth advantage is discussed. A parallel computational structure which implements the OBSCA is described and a system architecture is proposed.

| 20 DISTRIBUTION / AVAILABILITY OF ABSTRACT ☒ UNCLASSIFIED/UNLIMITED ☐ SAME AS RPT ☐ DTIC USERS | 21 ABSTRACT SECURITY CLASSIFICATION UNCLASSIFIED |
|---|---|
| 22a NAME OF RESPONSIBLE INDIVIDUAL LOOMIS, Herschel H., Jr. | 22b TELEPHONE (Include Area Code) (408)646-3214    22c OFFICE SYMBOL EC/Lm |

DD Form 1473, JUN 86     Previous editions are obsolete.     SECURITY CLASSIFICATION OF THIS PAGE

S/N 0102-LF-014-6603     UNCLASSIFIED

## IMPLEMENTATION OF THE
## ONE BIT SPECTRAL CORRELATION ALGORITHM

by

George A. Hutcheson
Lieutenant, United States Navy
B.S., Augusta College , 1984

Submitted in partial fulfillment
of the requirements for the degree of

## MASTER OF SCIENCE IN ELECTRICAL ENGINEERING

from the

## NAVAL POSTGRADUATE SCHOOL
June 1992

**ABSTRACT**

The computational efficiency of the *One Bit Spectral Correlation Algorithm* is compared to other cyclic spectrum analysis algorithms. A transmission bandwidth advantage is discussed. A parallel computational structure which implements the OBSCA is described and a system architecture is proposed.

**TABLE OF CONTENTS**

## LIST OF TABLES

# LIST OF FIGURES

# I. INTRODUCTION

## 1. BACKGROUND

### a. *SPECTRAL CORRELATION ANALYSIS*

Spectral correlation analysis is a method of signal analysis which takes advantage of the cyclostationary properties found in many communications signals. Most digital modulation schemes produce signals with underlying periodically time-variant structures. These structures give rise to observed functions of time which are successfully modelled as cyclostationary waveforms. This is especially true in connection with detection, estimation, synchronization, and emitter location. The *spectral correlation function*(SCF) is the cross spectrum of a signal with a time or frequency shifted version of itself. The SCF and cyclostationary waveform theories are discussed fully in references 1 through 6.

The SCF gives rise to the *cyclic cross spectrum*, a three dimensional plot of the signal on the bifrequency plane. Figure 1 shows the cyclic cross spectrum of a BPSK signal plotted on the bifrequency plane. The horizontal, or frequency, axis is denoted by $f_j$. The vertical axis is called the cyclic frequency axis and is denoted by $\alpha_i$. Each feature

1

on the plane lies along a line of constant $\alpha$. The large feature in the background is the normal signal power spectrum and lies along the $\alpha=0$ axis. The tallest feature in the foreground is twice the carrier frequency and the two closest features on either side are the data.

Because many modulated signals have a unique cyclic spectrum, cyclic spectrum analysis is particularly well suited for signal detection, modulation, recognition, signal parameter estimation, and the design of communication systems. However, cyclic spectrum analysis has a very high computational complexity which limits its use as a signal and systems analysis tool. The basic operations in cyclic spectrum analysis techniques are Fourier transformations, convolution, and product modulation which are common to most signal processing algorithms [Ref. 7]. The sheer number of calculations required for cyclic spectrum analysis far exceeds conventional spectral analysis and often proves too great for general purpose computers.

### b. METHODS OF COMPUTATION

In general, there are two broad categories of cyclic spectrum analysis algorithms: time-smoothing and frequency-smoothing techniques. Smoothing is the term used to describe the process by which unwanted irregularities are removed from the cyclic periodogram. The basic time and frequency

2

smoothing techniques are developed in reference 3. Time-smoothing techniques include the *FFT Accumulation Method (FAM)* and the *Strip Spectral Correlation Algorithm (SSCA)*. These methods were introduced in reference 4 and discussed in references 8 through 9. In reference 10, it is shown that these techniques are much more computationally efficient than the basic *Frequency Smoothing Method (FSM)*. This is because time smoothing techniques require less computations on the average than their frequency smoothing counterparts. However, reference 7 introduced the *One Bit Spectral Correlation Algorithm (OBSCA)*. OBSCA is a variation of FSM which has some interesting properties that offer attractive advantages over the less computationally intense time smoothing algorithms. Each of these algorithms perform the computations necessary to calculate the entire cyclic cross spectrum.

### c. *TDOA APPLICATION*

The *One Bit Spectral Correlation Algorithm* is particularly well suited for time difference of arrival applications. The two primary methods for computing the TDOA of a signal are the *Spectral Correlation Ratio Method* (SPECCORR) and the *Spectral Coherence Alignment Method* (SPECCOA). In both methods, a signal which is received at each of two receivers is needed to process the algorithms. The manner of computation each method employs is slightly different.

The algorithm for SPECCORR [Ref. 11] is

$$\hat{D} = \arg \max_{\tau} \{\hat{b}_\alpha(\tau)\} \tag{1}$$

where the argument is an estimate of

$$b_\alpha(\tau) \triangleq \left| \int_{||f| - \hat{f}_\alpha| < B_\alpha/2} \frac{S_{yx}^\alpha(f)}{S_x^\alpha(f)} e^{i2\pi f\tau} df \right|. \tag{2}$$

The algorithm for SPECCOA is

$$\hat{D} = \arg \max_{\tau} \{\hat{c}_\alpha(\tau)\} \tag{3}$$

and the argument is an estimate of

$$\hat{c}_\alpha = Re \left\{ \int_{|f| < B} S_{yx}^\alpha(f) S_x^\alpha(f)^* e^{i2\pi(f+\alpha/2)\tau} df \right\}. \tag{4}$$

As can be noted from the above equations, both SPECCORR and SPECCOA require the computation of $S_x$ in order to determine the location of any features of interest and then the computation of $S_{yx}$ along that $\alpha$ to perform the TDOA calculation. It is the calculation of $S_{yx}(f)$ for a specific $\alpha$ and all f where the OBSCA algorithm shows the most promise.

4

## 2. THESIS GOALS

This paper takes a closer look at OBSCA's unique properties and examines the potential advantages in computing the cyclic cross spectrum. Comparisons are made against the FAM and FSM algorithms on the basis of the *Hardware Complexity Product* [Ref. 10] for both the entire bifrequency plane and the special case where there is a specific cyclic frequency of interest. While SSCA is similar in performance to the FAM over the entire bifrequency plane, it cannot be simplified in a manner which is advantageous in calculating the special case of one $\alpha$ of interest. Therefore, only FAM and FSM will be used for comparison with OBSCA.

A highly parallel system architecture for OBSCA was proposed in reference 7. That architecture was proposed for the calculation of the entire cyclic cross spectrum. This paper analyzes the computation requirements for the algorithm and proposes a system architecture which incorporates those ideas in a manner which allows the OBSCA algorithm to be implemented so as to compute $S_x(f)$ and $S_{yx}(f)$ along a line of given $\alpha$.

## II. ONE BIT SPECTRAL CORRELATION ALGORITHM

### A. INTRODUCTION AND THEORY

The One Bit Spectral Correlation Algorithm is based on the *Digital Frequency Smoothing Method* of computing the cyclic cross spectrum. A frequency smoothed point estimate of the bifrequency plane at a point $(f_j, \alpha_i)$ is

$$S_{xy_{\Delta t}}^{\alpha_i}(f_j)_{\Delta f} = \frac{b(f_j, \alpha_i)}{M} \sum_{m=-M/2}^{M/2-1} X_{\Delta t}\left(j + \left\lfloor\frac{i}{2}\right\rfloor + m\right) \Phi\left[Y_{\Delta t}\left(j - \left\lceil\frac{i}{2}\right\rceil + m\right)\right]^*. \quad (5)$$

M is restricted to be an even integer. The scaling factor associated with equation (5) is

$$b(f_j, \alpha_i) = \frac{1}{2M} \sum_{m=-M/2}^{M/2} \Phi\left[Y_{\Delta t}\left(j - \frac{i}{2} + m\right)\right] Y_{\Delta t}^*\left(j - \frac{i}{2} + m\right). \quad (6)$$

The cyclic frequency coordinate is given by $\alpha_i = i/N$ and the spectral frequency coordinate is given by $f_j = j/N$. Where $N = \Delta t$ is the number of samples to be processed assuming a unity sampling rate. $X_{\Delta t}(k)$ and $Y_{\Delta t}(k)$ are Fourier transformations of the sampled sequences $x(n)$ and $y(n)$, which are derived, in turn, by sampling $x(t)$ and $y(t)$ at a rate of

$f_s$, assumed to be unity for subsequent developments. $Y(t)$ is generally a time shifted version of $x(t)$ such that $y(t) = x(t-t_0)$.

In order to compute the entire bifrequency plane, equations (5) and (6) will need to be applied to the whole plane in some efficient manner. As discussed in references 4 and 9, each point estimate in the plane has a region of support called a *Cyclic Spectrum Analyzer (CSA) cell*. The cells are approximated as a rectangular shape with the length determined by $\Delta f$ and the width by $\Delta \alpha$. It is shown in reference 12 that the frequency resolution $\Delta f = M/N$ and the cyclic frequency resolution $\Delta \alpha = 1/N$ [Ref. 12]. To determine the statistical reliability of a point estimate, the time-frequency resolution product, $\Delta t \Delta f = M$, must be much greater than one [Ref. 3].

The CSA cells are used to tile the bifrequency plane in such a manner that there is no overlap and that the gaps are minimized. This will ensure that for the entire collection interval, the point estimates will be calculated so that the CSA cells cover the whole cyclic cross spectrum. This requires that the CSA cells be contiguous and non-overlapping in both f and $\alpha$. [Ref. 12]

The entire cyclic cross spectrum [Ref. 7] is

$$S^{\alpha}_{xy\Delta f}(f)_{\Delta f} = \{S^{\alpha_i}_{xy\Delta t}(f_{(jM)})_{\Delta f} : -Q \leq i \leq Q, -R \leq j \leq R\} \tag{7}$$

where

$$Q = M - N, \qquad (8)$$

and

$$R = \lfloor \frac{N - M - |i|}{2M} \rfloor. \qquad (9)$$

Figure 2 illustrates such a pattern of CSA cells for ᴀf = 1/8 and ᴀtᴀf = 4. In most cases, meaningful estimation requires ᴀtᴀf ≥ 512. This is especially true for weaker signals down in the noise [Ref. 7]. However, ᴀf = 1/8 is often encountered in practice, since ᴀf need be no smaller than one half the bandwidth of the signal of interest, [Ref. 10].

The Φ[.] function in the OBSCA equation is a complex sign detector. This function is generally applied to the time or frequency shifted spectral sequence prior to the correlation computation. The output of the complex sign detector needs to be rotated $\pi/4$ radians in order to reduce the complex multiplies of the correlation computation to simple sign changes and data multiplexing operations. [Ref. 7]

Table 1 summarizes how all this works. Column 1 shows the four possible sign combinations for a complex number. Column 2 shows the sign bits clipped from the rest of the data. Column 3 rotates the sign bits by $\pi/4$ radians and column 4

| $\Phi[Y']$ | $SB(\Phi[Y'])$ | $\Phi[Y']e^{j\pi/4}$ | $(\Phi[Y']e^{j\pi/4})^*$ | $X(\Phi[Y']e^{j\pi/4})^*$ | $(\Phi[Y']e^{j\pi/4})Y'^*$ |
|---|---|---|---|---|---|
| (1,1) | (0,0) | (0,1) | (0,-1) | $(x_i,-x_r)$ | $(y_i,y_r)$ |
| (-1,1) | (1,0) | (-1,0) | (-1,0) | $(-x_r,-x_i)$ | $(-y_r,y_i)$ |
| (-1,-1) | (1,1) | (0,-1) | (0,1) | $(-x_i,x_r)$ | $(-y_i,-y_r)$ |
| (1,-1) | (0,1) | (1,0) | (1,0) | $(x_r,x_i)$ | $(y_r,-y_i)$ |

Table 1: OBSCA decoding array operation

takes the complex conjugate of column 3. Column 3 is needed in equation (6) while column 4 is used in equation (5). Column 5 demonstrates the multiplexing function of these sign bits as applied to an arbitrary complex signal X, $(x_r,x_i)$. Similarly for column 6 with an arbitrary complex signal Y, $(y_r,y_i)$. After the data is multiplexed by the appropriate decoding array it is passed on to two accumulators (one for the real and imaginary parts). These accumulators require M additions to complete an estimate and then the output is multiplied by the scaling factor associated with that CSA cell. Figure 3 is a basic block diagram of this process. [Ref. 7]

## B. ALGORITHMIC COMPARISONS

### 1. ENTIRE BIFREQUENCY PLANE

The *Hardware Complexity Product*, $p_{hu}*F_I$, [Ref. 10] is used as a measure of the relative complexity of a particular

architecture in the analysis of both FAM and FSM in computing the spectral correlation function. $P_{hu}$ is simply the number of hardware units needed to accomplish the given computations, while the *Factor of Real Time*, $F_T$, is used as an aid in characterizing the closeness to real time computations of each of the different methods.

$$F_T = \frac{computation\ time}{collect\ time} \ . \tag{10}$$

$P_{hu} * F_T = C_u / \Delta t$ where $C_u$ is the number of computations needed and $\Delta t$ is the total number of samples processed. The *Hardware Complexity Product* is useful because for real time calculations $F_T=1$, and $p_{hu}$ will then represent the total number of hardware units needed to operate in parallel to achieve real time. In the case where only one hardware unit is available, $p_{hu}=1$, the *Factor of Real Time* gives a objective view of the length of time needed to perform all the necessary computations. For convenience, all complex butterflies, multipliers, and adders will be assumed to be rate-1 and radix-2.

Tables 2 and 3 summarize the complexity analysis for the major sections of the FSM and FAM realizations, respectively [Ref. 10]. Because $S_x(f)$ is concerned only with real valued signals, the inherent symmetry of the function makes it necessary to calculate only the first quadrant of the bifrequency plane.

| (1 required) | | $N^2/4M$ required | |
| --- | --- | --- | --- |
| | FFT | Correlator | Summer |
| CBF | $(N/2)\log_2 N$ | — | — |
| Cpx Mpy | $(N/2)\log_2 N$ | $M$ | — |
| Cpx Add | $N\log_2 N$ | — | $M$ |
| Real Mpy | $2N\log_2 N$ | $4M$ | — |
| Real Add | $3N\log_2 N$ | $2M$ | $2M$ |

Table 2: Complexity summary for FSM

a. *FSM*

From Table 2, the number of real multiplies for the FSM algorithm over the entire bifrequency plane is

$$C_{rm} = 2N * LOG_2 N + \frac{N^2}{4M}(4M) \tag{11}$$

Remembering N=$\Delta$t and M=$\Delta$t$\Delta$f, equation (11) becomes

$$C_{rm} = 2\Delta t * LOG_2 \Delta t + (\Delta t)^2 \tag{12}$$

and therefore

$$p_{rm} * F_T = \frac{C_{rm}}{N} = 2 LOG_2 \Delta t + \Delta t \tag{13}$$

Also from Table 2, the equation for the number of real additions for FSM is

$$C_{ra} = 3N * LOG_2 N + \frac{N^2}{4M}(4M) \tag{14}$$

and the *Hardware Complexity Product* becomes

11

$$p_{ra}*F_T = 3*LOG_2\Delta t + \Delta t \tag{15}$$

| | (P required) | | | ((N')^2/4 required) | |
|---|---|---|---|---|---|
| | Wndw | $N'$ FFT. | Down Convt. | Correl. Multi. | $P$ FFT |
| CBF | — | $(N'/2)\log_2 N'$ | — | — | $(P/2)\log_2 P$ |
| Cpx Mpy | — | $(N'/2)\log_2 N'$ | $N'$ | $P$ | $(P/2)\log_2 P$ |
| Cpx Add | — | $N'\log_2 N'$ | — | — | $P\log_2 P$ |
| Real Mpy | $N'$ | $2N'\log_2 N'$ | $4N'$ | $4P$ | $2P\log_2 P\cdot$ |
| Real Add | — | $3N'\log_2 N'$ | $2N'$ | $2P$ | $3P\log_2 P$ |

Table 3: Complexity summary for FAM

*b.  FAM*

Similarly, from Table 3, the number of real multiplies for FAM over the entire plane is

$$C_{rm} = 8N*LOG_2\frac{N}{M} + 2\frac{N^2}{M}*LOG_2 4M + 4\frac{N^2}{M} + 20N \tag{16}$$

and so the *Hardware Complexity Product* becomes

$$p_{rm}*F_T = 8*LOG_2\left(\frac{1}{\Delta f}\right) + 2\left(\frac{1}{\Delta f}\right)*LOG_2 4\Delta t\Delta f + 4\left(\frac{1}{\Delta f}\right) + 20 \tag{17}$$

The number of real additions for FAM are also taken from Table 3.

$$C_{ra} = 12N*LOG_2\frac{N}{M} + 3\frac{N^2}{M}*LOG_2 4M + 2\frac{N^2}{M} + 8 \tag{18}$$

Therefore

$$p_{ra}*F_T = 12*LOG_2\left(\frac{1}{\Delta f}\right) + 3\left(\frac{1}{\Delta f}\right)*LOG_2 4\Delta t\Delta f + 2\left(\frac{1}{\Delta f}\right) + 8 \qquad \textbf{(19)}$$

### c.   OBSCA

For OBSCA, the calculations are not as straightforward. Similarly to the calculations for FSM, the number of real multiplies for OBSCA is $C_{rm} = 4(C_{BF}+C_s)$, where $C_{BF}$ is the number of complex butterflies and $C_s$ is the number of scaling factors required over the bifrequency plane. The factor of 4 is due to the fact that each scaling factor is a complex quantity which must be multiplied to its respective CSA cell, and there are 4 real multiplies to each complex one. For the entire bifrequency plane, the number of scaling factors is given by

$$C_s = \frac{1}{2}\left(\frac{N}{M}\right)^2 - \frac{N}{M} + 1 \qquad \textbf{(20)}$$

However, due to the fact that the other two algorithms are computed only for the first quadrant of the bifrequency plane, the factor of 4 applied to $C_s$ is canceled. Therefore, the *Hardware Complexity Product* for OBSCA becomes

$$p_{rm}*F_T = \frac{C_{rm}}{N} = 2*LOG_2\Delta t + \frac{1}{2}\frac{1}{\Delta t\Delta f^2} - \left(\frac{1}{\Delta t\Delta f}\right) + \left(\frac{1}{\Delta t}\right) \qquad \textbf{(21)}$$

13

The number of real additions for OBSCA is $C_{ra}=6C_{BF}+2C_s+C_{sum}$, where $C_{sum}$ is the total number of additions required in all the accumulators over the entire bifrequency plane. From equation (5), there are M additions for each change in either i or j. So, from equation (3), $C_{sum}=M*$[range of i]*[range of j] = M*2Q*2R, or

$$C_{sum}=M(2(N-M))\left(2\left(\frac{N-M-|i|}{2M}\right)\right)=2(N-M)(N-M-|i|) \qquad (22)$$

Let i=0 in order to calculate the worst case total of operations. Then

$$C_{sum}=2(N-M)^2=2(N^2-2NM+M^2)=2N^2-4NM+2M^2 \qquad (23)$$

$$2C_s=2\left(\frac{1}{2}\left(\frac{N}{M}\right)^2-\frac{N}{M}+1\right)=\left(\frac{N}{M}\right)^2-2\frac{N}{M}+2 \qquad (24)$$

So the total of real additions for OBSCA is

$$C_{ra}=3N*LOG_2N+2N^2-4NM+M^2+\left(\frac{N}{M}\right)^2-2\frac{N}{M}+2 \qquad (25)$$

Again, removing a factor of 4 from $C_s$ and $C_{sum}$ to indicate the number of calculations in the first quadrant only

$$p_{ra}*F_T=3*LOG_2\Delta t+\frac{1}{2}\Delta t-\Delta t\Delta f+\frac{1}{4}(\Delta t\Delta f)^2+\frac{1}{4}\frac{1}{\Delta t\Delta f^2}-\frac{1}{2}\left(\frac{1}{\Delta f}\right)+\frac{1}{2}. \qquad (26)$$

Figures 4 and 5 illustrate the relationships between these equations quite clearly. The *Hardware Complexity Product* is plotted against the time-frequency resolution product in a log vs. log fashion. This shows that although there is enormous savings in the number of real multiplies, OBSCA is still not as advantageous as FAM over the whole plane. The low number of real multiplies is offset by the exponential increase in the number of real additions as $\Delta t \Delta f$ increases.

## 2. SINGLE CYCLIC FREQUENCY OF INTEREST

For applications such as Time difference of arrival, Frequency Difference of Arrival, signal classification, and parameter measurement, it is useful to look at a particular feature on the bifrequency plane. So, instead of computing the first quadrant of the plane, there are many situations where it is necessary to perform only those calculations needed for a single $\alpha_0$ and all $f_j$. Such situations include looking for a feature occurrence at a known $\alpha$, as well as using SPECCORR or SPECCOA to measure the time difference of arrival.

### a. FSM

The number of calculations due to the complex butterflies will not change. While the following equations are again discussed in terms of the first quadrant of the bifrequency plane, if $S_{xy}(f)$ is going to be calculated for

15

SPECCORR or SPECCOA, it will be necessary to include the negative frequencies also. Equations (23) through (34) can be easily adjusted by multiplying all but the first term by a factor of 2.

So, the number of real multiplies for FSM along a given $\alpha_0$ is

$$C_{rm}=2N*LOG_2N+\frac{N}{2M}(4M) \qquad (27)$$

and

$$p_{rm}*F_T=\frac{C_{rm}}{N}=2*LOG_2\Delta t+2 \qquad (28)$$

The number of real additions is given by

$$C_{ra}=3N*LOG_2N+\frac{N}{2M}(4M) \qquad (29)$$

and

$$p_{ra}*F_T=3*LOG_2\Delta t+2 \qquad (30)$$

### b. FAM

A similar argument follows for FAM. The number of calculations performed by the complex butterflies remains unchanged. The number of calculations required along one dimension of the bifrequency plane reduces from $(N')^2/4$ down

to just N'/2.  With N'=N/M, the single $\alpha$ calculations becomes
N/(2M).   And  the  number  of  real  multiplies  reduces  from
equation (12) to

$$C_{rm} = 8N * LOG_2 \frac{N}{M} + 4N * LOG_2 4M + 28N \qquad (31)$$

and

$$p_{rm} * F_T = 8 * LOG_2 (\frac{1}{\Delta f}) + 4 * LOG_2 4 \Delta t \Delta f + 28 \qquad (32)$$

The same reduction is apparent for the real additions,

$$C_{ra} = 12N * LOG_2 \frac{N}{M} + 6N * LOG_2 4M + 12N \qquad (33)$$

and therefore

$$p_{ra} * F_T = 12 * LOG_2 (\frac{1}{\Delta f}) + 6 * LOG_2 4 \Delta t \Delta f + 12 \qquad (34)$$

### c.   OBSCA

Along  a  single  line  of  $\alpha$,  the  OBSCA  calculation  for
positive f is relatively simple.  The number of operations due
to  the  complex  butterflies  is  the  same  as  FSM.    While  the
relationship  for  the  real  multiplies  is  exactly  the  same  as
for  the  whole  plane  $C_{rm} = 4(C_{BF} + C_s)$,  $C_s$  is  now  much  less.    The
largest  number  of  scaling  factors  is  along  the  f  axis  where

17

$\alpha_0=0$. In this case, for single $\alpha$ and positive f, $C_s=0.5[(N/M)-1]$. So

$$C_{rm}=2N*LOG_2N+2\frac{N}{M}-2 \qquad (35)$$

and

$$p_{rm}*F_T=\frac{C_{rm}}{N}=2*LOG_2\Delta t+2\left(\frac{1}{\Delta t\Delta f}\right)-2\left(\frac{1}{\Delta t}\right) \qquad (36)$$

The formula for real additions is also the same, $C_{ra}=6C_{BF}+2C_s+C_{sum}$. But $C_{sum}$, as well as $C_s$, is different. In equation (5), there are M additions for each i and j. Here i is a constant. From equation (7), then, $C_{sum}=M*[range of j]=2MR$. With i=0, and substituting equation (9) for R, $C_{sum}=N-M$. And for positive f, $C_{sum}=0.5(N-M)$. Also, $2C_s=2\{0.5[(N/M)-1]\}=(N/M)-1$. Therefore, the total number of real additions is

$$C_{ra}=3N*LOG_2N+\frac{N-M}{2}+\left(\frac{N}{M}\right)-1 \qquad (37)$$

and

$$p_{ra}*F_T=3LOG_2\Delta t+\frac{1}{2}-\frac{1}{2}\Delta f+\left(\frac{1}{\Delta t\Delta f}\right)-\left(\frac{1}{\Delta t}\right) \qquad (38)$$

It is important to notice that because the double summation in equation (7) is reduced to a single summation for

18

a given $\alpha_0$, the number of real additions has only a factor of N in the second term of equation (37) instead of the $N^2$ in equation (25). This factor then drops completely out of equation (38). This rids OBSCA of that exponential rise in the number of real additions which is the reason that the algorithm is not competitive in calculating the whole bifrequency plane. It is also interesting to note that equation (38) is not significantly less than equation (26) for FSM. Especially in light of the fact that the last three terms in equation (34) are considerably less than one and can be ignored compared to the first two terms. Thus, it is surprising to see that FSM is extremely competitive with OBSCA in computing the a single line of $\alpha$.

Figures 6 and 7 show the *Hardware Complexity Product* of the real multiplications and real additions for a single $\alpha$, respectively. As in Figures 4 and 5, these are plotted against the time-frequency resolution product in order to better display the tendencies for useful ᴧtᴧf's. As shown, OBSCA is much more efficient than FAM for a single $\alpha$, but it is also shown how close FSM is to OBSCA.

## C. BANDWIDTH ADVANTAGE

Because of the manner in which OBSCA is calculated, there is an advantage in using OBSCA in TDOA calculations. The two methods, SPECCORR and SPECCOA, require that both the auto-correlation, $S_x(f)$, and the cross correlation, $S_{yx}(f)$, be

19

computed. OBSCA can reduce the amount of data which needs to be transferred. Under normal circumstances, two separate receivers are used to receive the signals. For the sake of argument, let receiver one (R1) receive the signal $x(t)$ and perform the computations, and receiver two (R2) receive the time shifted signal $x(t-t_0)=y(t)$. In order for R1 to implement the SPECCOA algorithm, R2 must send all N sample of complex data to R1. Let n be the number of bits required for each real and imaginary parts. Then, R2 must send 2Nn bits of data. R1 can then compute $S_{xy}$ and $S_x$ for the SPECCOA algorithm.

Examination of equation (5) reveals that the complex sign detector function, $\Phi[.]$, only relies on the spectral data from $y(t)$, while equation (6) shows that the scaling factors can also be computed solely from this same data. Therefore, in a similar situation where R1 receives $x(t)$ and R2 receives $y(t)$, the transmission bandwidth required is less by at least a factor of 10. Once both signals are received, R1 can determine the cyclic frequency of interest. This is sent to R2 using n bits. R2 can now calculate the required scaling factors and clip the sign bits from the spectral data of $y(t)$. At most there are $(N/M)-1$ scaling factors along the f axis [Ref. 7]. Since these are complex numbers, this is sent to R1 with $((N/M)-1)2n$ bits. The resulting sign bits for N samples only need 2N bits to be sent to R1. The total number of bits required to transmit all this data back and forth is

$n_t = (2Nn)/M + 2N + n$ bits for OBSCA as opposed to $2Nn$ bits normally. Typical values are N=4,194,304, M=4096, and n=24 bits. These numbers lead to an approximate reduction of 25 times less data needing to be transmitted. This is illustrated clearly in Figure 8.

While the $\Phi[.]$ data only has to be transmitted once, each $\alpha$ must be sent separately. Furthermore, if these $\alpha$'s are not sufficiently close so as to fall within the same set of partitions, then a new set of scaling factors must be sent as well. This, of course, would increase the required bandwidth necessary to transmit the data.

# III.   STRUCTURES FOR SINGLE CYCLIC FREQUENCIES

## A.   INTRODUCTION

Reference 7 introduces a structural architecture which allows highly parallel computational implementations of the OBSCA in calculating the entire bifrequency plane.  In order to accomplish this, reference 7 describes a *Basic Partitioning Scheme* (BPS) which mimics the contiguous and nonoverlapping pattern of CSA cells in Figure 2.  The idea is that once the bifrequency plane has been appropriately tiled with partitions based on the BPS, all the calculations within each partition can be conducted independently of any other partition.  Each partition on the plane is mapped into a square array called the **Q** array.  This array is then subdivided into related partitions called the **R** and **S** arrays.  These arrays in turn led to a suggestion of an architecture for parallel computation.  The example in reference 7 uses $\Delta f = 1/8$ which is achieved with N=16 and M=2.  The number of partitions from equation (20) is $C_s = 25$.  These partitions map into the **Q** array as shown in Figure 9, and Figure 10 shows how the **R** and **S** arrays are formed from the **Q** array.  Taking the R array as a further example, reference 7 goes on to show that if processor elements were arranged as in Figure 11, each partition would

be computed in parallel. Further parallelism within each processor element was also discussed.

## B. EQUIVALENT STRUCTURE FOR SINGLE CYCLIC FREQUENCY OF INTEREST

Continuing with the concept that it would be advantageous at times to calculate a line of frequency for a given cyclic frequency of interest, the following structure is presented. Based on the ideas found in reference 7, only minor modifications need to be made to allow highly parallel computation of a single $\alpha_0$.

The architecture in reference 7 is shown in Figure 12. Since each partition requires a contiguous band of spectral data, the process begins by transferring the spectral data from the output of the FFT's to the X and Y memory buffers of the processor element. The data is broadcasted sequentially from one end of the spectral band to the other and the memory buffers intercept and store its appropriate band of data. Once all this is accomplished, all the partitions are computed simultaneously.

Upon examining Figures 11 and 12 closely, it is of interest to note that for a given $\alpha$, the X and Y memory buffer are only used, at most, once each. This readily suggests that a decoding array can be implemented which uses $\alpha$ as an input and multiplexes the X and Y memory buffers appropriately to compute the correct partitions associated with the given $\alpha$.

Figure 13 shows the R and S arrays with the X and Y memory buffers. Figure 14 shows how a given α fixes the use of each X and Y memory buffer to calculate the partitions for Δf=1/8. Once each partition is computed, it is passed on to be scaled as needed. Within each processor element, the same architecture suggested in reference 7 can be used without modification.

The advantage in this structure, of course, is that there are not so many processor elements needed to perform the desired calculations. At most, (N/M)-1 processor elements would be required as mentioned earlier. Although it would be infrequently required to calculate along the f axis as that is the normal signal power spectrum, if less processor elements were used it would be possible not to have enough elements to calculate all the required partitions in a single pass. This would require that some processor elements compute more than one partition which obviously slows performance and defeats the advantages inherent in the parallel design.

# IV. SUMMARY

## A. CONCLUSIONS

The multiplexing properties of the OBSCA allow for greatly reduced numbers of real multiplications. However, it is not sufficient to give OBSCA an advantage over the better time smoothing algorithms. FAM and SSCA are still far more computationally efficient in computing the entire bifrequency plane than their frequency smoothing counterparts, even with OBSCA.

It has been shown that OBSCA is much better suited for calculating a single $\alpha$ than either FAM or SSCA. However, it is interesting to note that while OBSCA is intended to increase the computational efficiency of the frequency smoothing methods, the direct application of the FSM proved to be nearly as efficient as OBSCA.

There does exist a transmission bandwidth advantage to using OBSCA in TDOA operations. This is especially true when there are multiple cyclic frequencies of interest within the same set of partitions. The advantage is diminished slightly for each new $\alpha$ which lies in a new partition set.

Application specific integrated circuits appears to be a natural implementation procedure for the proposed system architecture illustrated in Figures 11, 12, and 14.

25

## B. RECOMMENDATIONS

In the case where there is only one cyclic frequency of interest, it is readily apparent from this research that a closer study of FSM and OBSCA is required to understand the trade offs between the two methods. It is, therefore, recommended that further analysis be conducted concentrating on the computational and implementational similarities and differences that exist between FSM and OBSCA.

Further architectural study is needed to determine a suitable Application Specific Integrated Circuit (ASIC) which would be appropriate to OBSCA. The OBSCA's obvious potential of implementation using massively parallel architectures far exceeds that of the other algorithms and also requires a more in depth approach than given here.
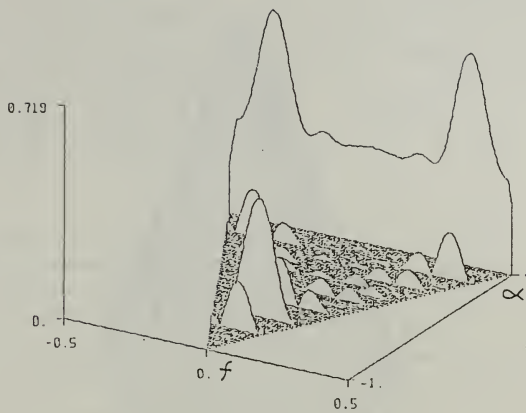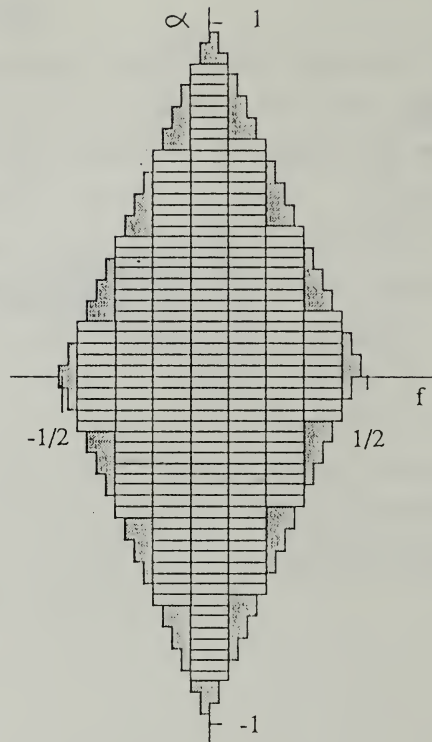
**Figure 1** BPSK signal on bifrequency plane

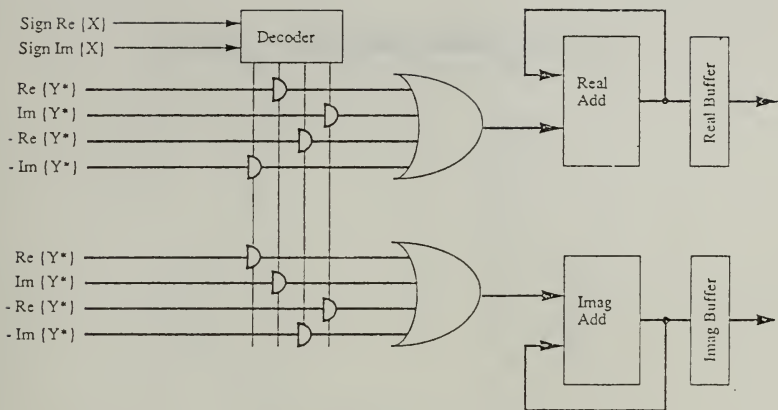**Figure 2** CSA cells tiling the bifrequency plane

28

**Figure 3** Arithmetic unit for OBSCA

29
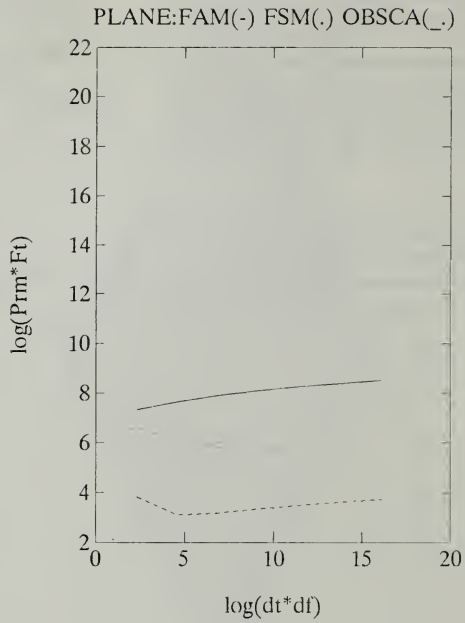
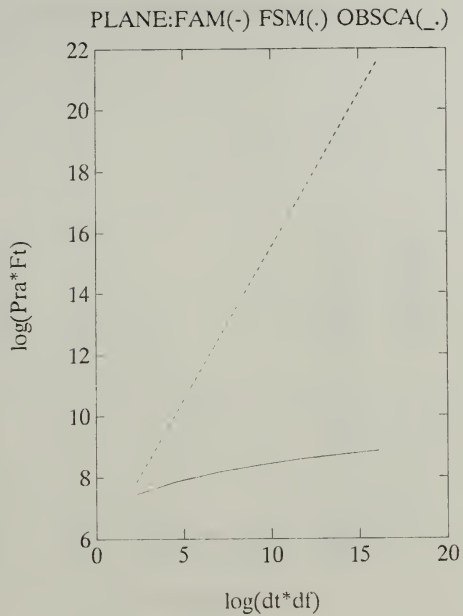**Figure 4** Complexity of real multiplies for entire plane

PLANE:FAM(-) FSM(.) OBSCA(_.)

**Figure 5** Complexity of real adds for entire plane

31

ALPHA:FAM(-) FSM(.) OBSCA(_.)
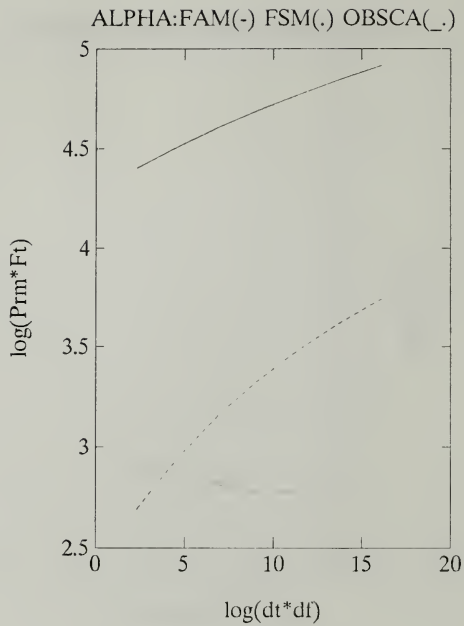
Figure 6 Complexity of real multiplies for single α
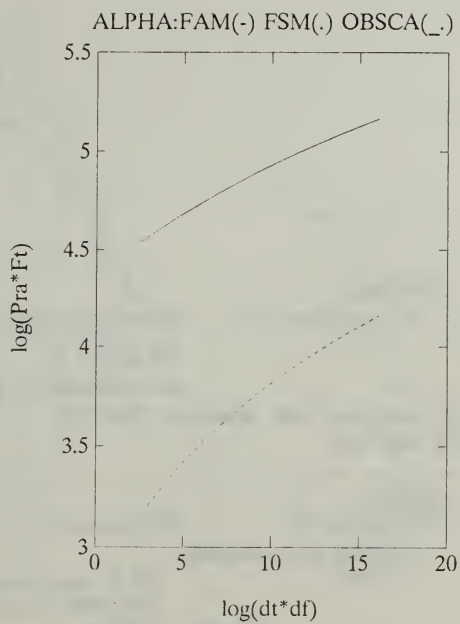
**Figure 7** Complexity of real adds for single $\alpha$

**Normally**

R1 receives x(t) | R2 receives y(t)

R2 sends all
spectral data to R1

R1 computes both ⟸ 2Nn bits
$S_x$ and $S_{yx}$

**OBSCA**

R1 receives x(t) | R2 receives y(t)

ALPHA sent ⟹
(n bits)  $\overline{\Phi}[:]^*$ are computed
and need be sent once
⟸ 2N bits

And then
R1 computes both | all scaling factors for the
$S_x$ and $S_{yx}$ | partitions associated with
each alpha sent over

⟸ $\dfrac{N}{M}$ - 2n bits
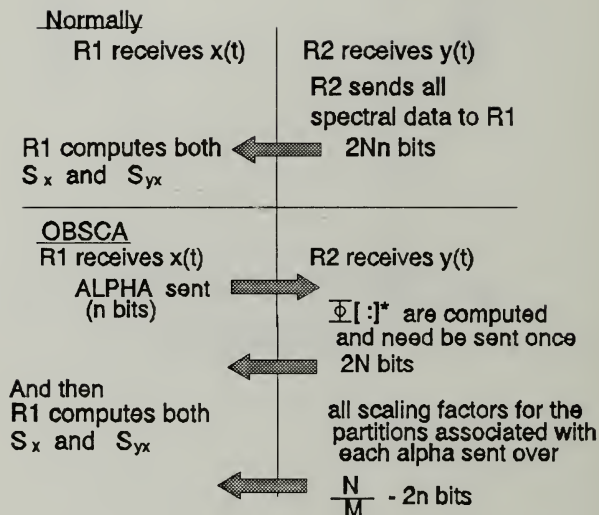
**Figure 8** Comparison of required transmission bandwidths

34

The Q Array

P[-3,0]      P[-2,1]      P[-1,2]      P[0,3]

P[-2,0]      P[-1,1]      P[0,2]

P[-2,-1]      P[-1,0]      P[0,1]      P[1,2]

P[-1,-1]      P[0,0]      P[1,1]

P[-1,-2]      P[0,-1]      P[1,0]      P[2,1]

P[0,-2]      P[1,-1]      P[2,0]

P[0,-3]      P[1,-2]      P[2,-1]      P[3,0]
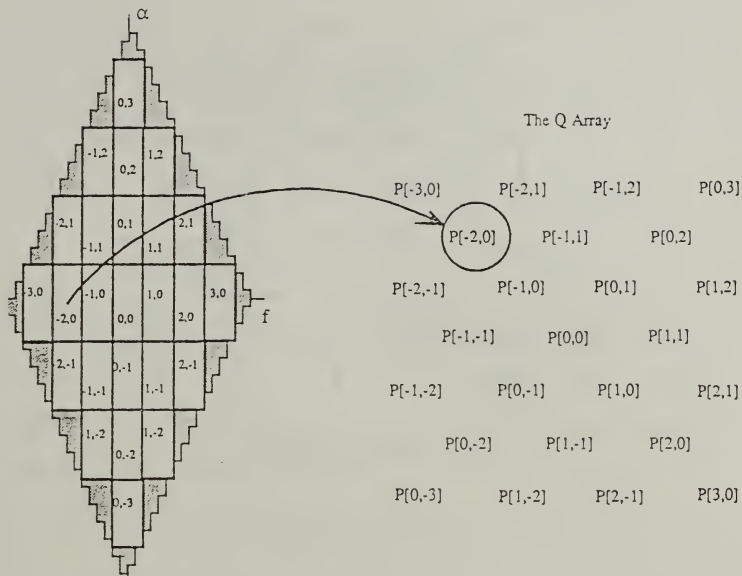
**Figure 9** Mapping of the BPS into the Q array

The Q Array

The R Array

The S Array
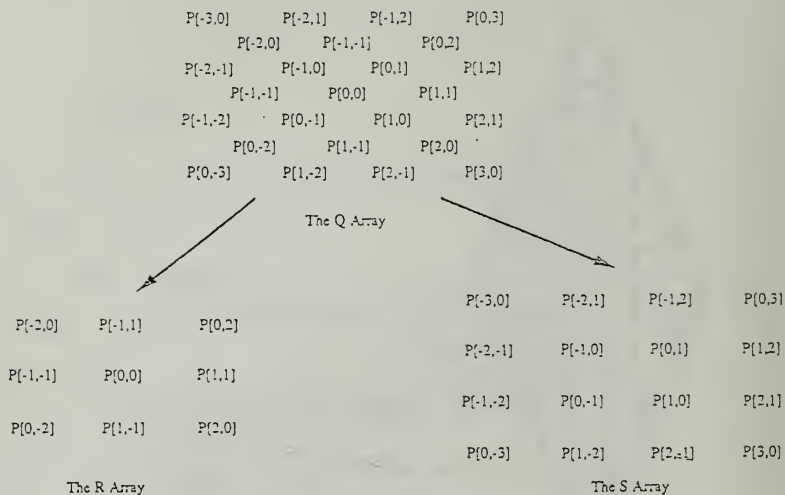
**Figure 10** Decomposition of Q array into R and S arrays
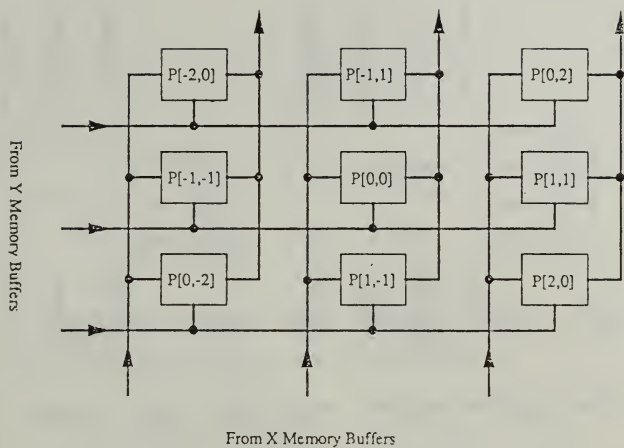
From X Memory Buffers

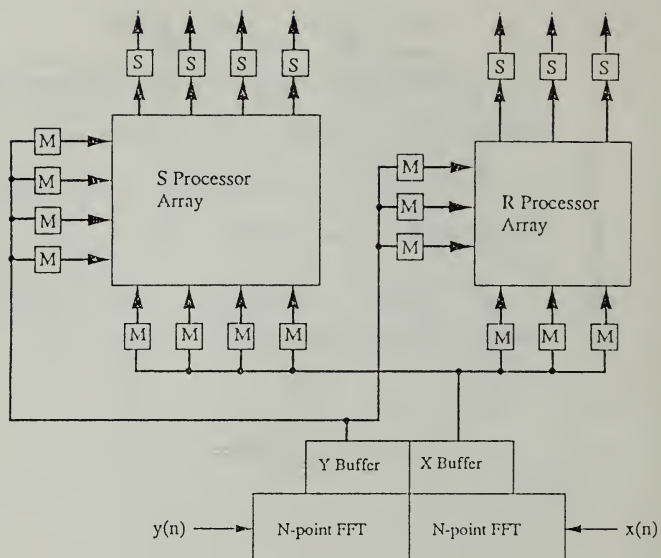**Figure 11** The R processor array

37

**Figure 12** System architecture for $\Delta f = 1/8$
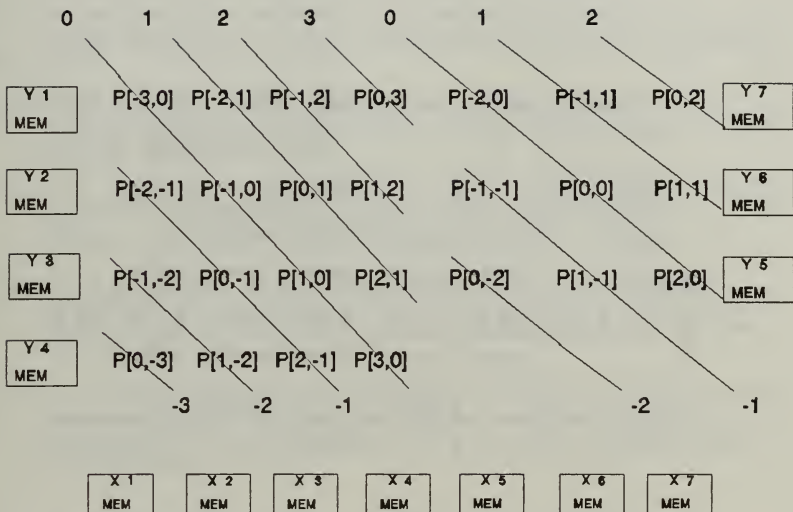
**Figure 13** The R and S arrays with aligned memory buffers

39

|  | PE 1 | PE 2 | PE 3 | PE 4 | PE 5 | PE 6 | PE 7 |
| --- | --- | --- | --- | --- | --- | --- | --- |
| f= | -3 | -2 | -1 | 0 | 1 | 2 | 3 |
| -3 |  |  |  | X1 Y4 |  |  |  |
| -2 |  |  | X1 Y3 | X5 Y5 | X2 Y4 |  |  |
| -1 |  | X1 Y2 | X5 Y6 | X2 Y3 | X6 Y5 | X3 Y4 |  |
| 0 | X1 Y1 | X5 Y7 | X2 Y2 | X6 Y6 | X3 Y3 | X7 Y5 | X4 Y4 |
| 1 |  | X2 Y1 | X6 Y7 | X3 Y2 | X7 Y6 | X4 Y3 |  |
| 2 |  |  | X3 Y1 | X7 Y7 | X4 Y2 |  |  |
| 3 |  |  |  | X4 Y1 |  |  |  |

(Left side vertical label: A L P H A)

**Figure 14** Single α decoding array

## LIST OF REFERENCES

[1]  W. A. Gardner,"The spectral correlation theory of cyclostationary time-series,"*Signal Processing*, vol.11,pp. 13-36,July 1986.

[2]  W. A. Gardner,"Measurement of spectral correlation,"*IEEE Trans. Acoust., Speech, Signal Processing*,vol. ASSP-34,pp. 1111-1123, October 1986.

[3]  W. A. Gardner, *Statistical Spectral Analysis: A Nonprobabilistic Theory*, Englewood Cliffs,NJ:Prentice-Hall,1987.

[4]  W. A. Brown,"On the theory of cyclostationary signals,"Ph.D. dissertation, University of California, Davis, September 1987.

[5]  W. A. Gardner,"Spectral correlation of modulated signals, part I — Analog modulation," *IEEE Trans. on Communications*, vol. COM-35,pp. 584-594, June 1987.

[6]  W. A. Gardner, W. A. Brown, and C. K. Chen,"Spectral correlation of modulated signals, part II — Digital modulation," *IEEE Trans. on Communications*, vol. COM-35,pp. 595-601, June 1987.

[7]  R. S. Roberts and H. H. Loomis, Jr.,"Parallel computation structures for a class of cyclic spectral analysis algorithms,"submitted to *IEEE Transactions on Signal Processing*.

[8]  W. A. Gardner and H. H. Loomis, Jr.,"Digital implementations of spectral correlation analyzers," *IEEE Fourth Annual ASSP Workshop on spectrum Estimation and Modeling*,pp. 264-270, August 1988.

[9]  R. S. Roberts, W. A. Brown, and H. H. Loomis, Jr.,"Computationally efficient algorithms for cyclic spectral analysis," *IEEE Signal Processing Magazine*, vol. 8, No. 2, pp. 38-49, April 1991.

[10] W. A. Brown and H. H. Loomis, Jr.,"Digital implementations of spectral correlation analyzers,"*IEEE Transactions on Signal Processing*, Spring 1993,(in press).

[11] C. Chih-Kang and W. A. Gardner,"Signal-selective time-difference-of-arrival estimation for passive location of manmade signal sources in highly corruptive environments. Part II: algorithms and performances," *IEEE Transactions on Signal Processing*,vol. 40,1992(in press).

[12] R. S. Roberts,"Architectures for digital cyclic spectral analysis," Ph.D. dissertation, Department of Electrical Engineering and Computer Science, University of California, Davis, 1989.

# INITIAL DISTRIBUTION LIST

1.  Defense Technical Information Center                          2
    Cameron Station
    Alexandria, Virginia 22304-6145

2.  Library, Code 52                                             2
    Naval Postgraduate School
    Monterey, California 93943-5002

3.  Chairman, Code EC                                            1
    Department of Electrical and Computer Engineering
    Naval Postgraduate School
    Monterey, California 93943-5000

4.  Prof. H. Loomis, Code EC/Lm                                 4
    Department of Electrical and Computer Engineering
    Naval Postgraduate School
    Monterey, California 93943-5000

5.  Prof. R. Bernstein, Code EC/Be                              1
    Department of Electrical and Computer Engineering
    Naval Postgraduate School
    Monterey, California 93943-5000

6.  LT George A. Hutcheson                                      1
    344 Folkstone Circle
    Augusta, Georgia 30907

7.  Randy S. Roberts                                            1
    Signal Processing Group
    Department of Electrical Engineering and Computer Science
    University of California
    Davis, California 95616